

NJC

Accepted Manuscript



This is an *Accepted Manuscript*, which has been through the Royal Society of Chemistry peer review process and has been accepted for publication.

Accepted Manuscripts are published online shortly after acceptance, before technical editing, formatting and proof reading. Using this free service, authors can make their results available to the community, in citable form, before we publish the edited article. We will replace this *Accepted Manuscript* with the edited and formatted *Advance Article* as soon as it is available.

You can find more information about *Accepted Manuscripts* in the [Information for Authors](#).

Please note that technical editing may introduce minor changes to the text and/or graphics, which may alter content. The journal's standard [Terms & Conditions](#) and the [Ethical guidelines](#) still apply. In no event shall the Royal Society of Chemistry be held responsible for any errors or omissions in this *Accepted Manuscript* or any consequences arising from the use of any information it contains.



www.rsc.org/njc

ARTICLE

Heterometallic coordination polymers: Syntheses, structures and heterogeneous catalytic applications

Cite this: DOI: 10.1039/x0xx00000x

Deepak Bansal,^a Saurabh Pandey,^a Geeta Hundal,^b and Rajeev Gupta^{a*}

Received 00th January 2012,

Accepted 00th January 2012

DOI: 10.1039/x0xx00000x

www.rsc.org/

A metalloligand Na[Co(L¹)₂] (**1**) of ligand H₂L¹ (N2,N6-bis(4,5-dihydrothiazol-2-yl)pyridine-2,6-dicarboxamide) offering appended thiazoline rings has been used for the synthesis of one-dimensional {Co³⁺-Zn²⁺} (**2**), {Co³⁺-Cd²⁺} (**3**) and {Co³⁺-Hg²⁺} (**4**) coordination polymers. **1** offers appended thiazoline rings having both soft, sulphur, as well as hard, nitrogen, donors. The crystal structures of **2** and **3** display the coordination of hard thiazoline-N donors to the Zn²⁺ and Cd²⁺ ions. Interestingly, **4** illustrates the bonding through both hard thiazoline-N as well as soft thiazoline-S donors. The three heterometallic coordination polymers have been used as the reusable heterogeneous catalysts for the ring-opening reactions of oxiranes and thiiranes; Knoevenagel condensation of benzaldehydes and benzothialdehydes; and cyanation reactions of aldehydes and carbothialdehydes. Our results demonstrate that the relative size and Lewis acidity of secondary metals potentially control the catalysis outcome via preferential interaction with the substrates.

Introduction

In recent years, rational design and construction of new inorganic-organic hybrid materials has been an active research field.¹⁻⁴ In this context, utilization of coordination complexes as the metalloligands offers several advantages of producing materials including fair amount of predictability and therefore tailor-made architectures.¹ Importantly, such materials not only offer fascinating structural topologies⁵⁻⁸ but important applications in sorption,⁹ separation,¹⁰ ion-exchange,¹¹ proton conduction,¹² optics,¹³ magnetism,¹⁴ luminescence¹⁵ and catalysis.¹⁶ Our group has developed several metalloligands offering assorted appended functional groups.¹⁷⁻²² Such appended functional groups have been shown to coordinate a variety of secondary metal ions producing assorted materials. While metalloligands offering appended pyridyl groups have afforded hetero-trimetallic complexes¹⁸ as well as two-(2D) and three-dimensional (3D) networks;¹⁹ thiazole-appended metalloligands have been able to introduce hydrogen bonds (H-bonds) in close proximity of the secondary metals in the resultant coordination polymers.²²

Preferential interaction of a substrate to a catalytic metal center is a *key-step* in the metal-mediated organic transformations.^{23a,23b} Despite the availability of a significant amount of spectroscopic, kinetic, and theoretical data to understand such a vital step, detailed structural and mechanistic information is still lacking.^{23c-23f} Although extensive attempts have been made to comprehend the activation of a substrate during the catalysis, the molecular-level details are still in early stage.^{23c} For example, Lewis acidity of a metal ion depends on

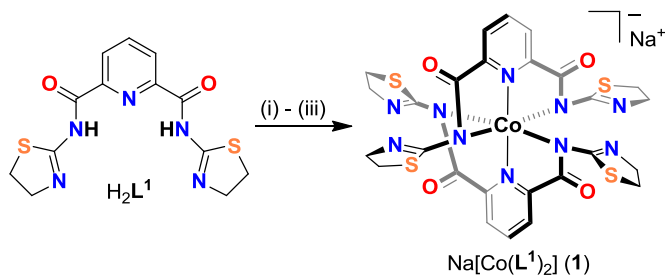
several factors including size and charge of the cation.²⁴ Ideally, a decent control on two such essential components, charge and size, provides an option to control the Lewis acidity of a metal ion and therefore its preference to interact and/or bind a substrate. In past, we have shown a set of hetero-trimetallic complexes having Zn(II), Cd(II), and Hg(II) ions as the secondary catalytic sites where a difference of Lewis acidity of the respective cation was found to control the substrate activation step and subsequently the reactivity.^{18b} Herein, we show the utilization of thiazoline-appended metalloligand of ligand H₂L¹ (N2,N6-bis(4,5-dihydrothiazol-2-yl)pyridine-2,6-dicarboxamide) in the synthesis of one-dimensional (1D) coordination polymers. These coordination polymers, containing Zn(II), Cd(II), and Hg(II) ions as the catalytic sites, act as the heterogeneous catalysts for the ring-opening reactions of oxiranes and thiiranes; Knoevenagel condensations of benzaldehydes and benzothialdehydes; and cyanation reactions of aldehydes and carbothialdehydes. Our results illustrate that the difference in the size and Lewis acidity of secondary metals potentially controls the catalysis outcome via preferential interaction with the substrates.

Results and discussion

Synthesis and characterization of metalloligand **1**

The metalloligand Na[Co(L¹)₂] (**1**) was synthesized by the reaction of deprotonated ligand [L¹]²⁻ (where H₂L¹ = N2,N6-bis(4,5-dihydrothiazol-2-yl)pyridine-2,6-dicarboxamide) with Co(II) salt followed by oxidation using O₂ (Scheme 1). Complex **1** shows red-shifted ν_{amide} stretches at 1618 cm⁻¹

suggesting the bonding through deprotonated N_{amide} group which is further corroborated by the absence of ligand's $\nu_{\text{N-H}}$ stretches.^{25a} The conductivity data confirms the 1:1 electrolytic nature.^{25b} The ^1H NMR spectrum of **1** exhibits thiazoline ring protons as triplets at 2.7 and 3.0 ppm whereas pyridine ring protons were observed as doublet and triplet at ca. 8.0 and ca. 8.4 ppm, respectively (Fig. S1 and S2, ESI). The DMF solution of **1** displays λ_{max} at 670 nm in addition to a shoulder at 472 nm (Fig. S3, ESI). Metalloligand **1** was crystallographically characterized and its molecular structure is shown in figure 1. The structure shows that two tridentate ligands coordinate the Co^{3+} ion meridionally. Such a coordination mode leaves the appended thiazoline rings uncoordinated as noted with our earlier metalloligands offering appended pyridine or thiazole rings.^{18,22} The Co^{3+} ion is coordinated to four N_{amide} donors in the basal plane whereas two N_{pyridine} rings occupy the axial positions. The geometry around the Co^{3+} ion is compressed octahedral wherein $\text{Co}-N_{\text{amide}}$ distances (avg. 1.954 Å) are longer than that of $\text{Co}-N_{\text{pyridine}}$ distances (avg. 1.880 Å) although within the range as observed before.^{18,21,26} The solid-state packing of **1** shows that the complex anions are connected via appended thiazoline rings to the Na^+ cations ($\text{Na}-\text{N4}$: 2.531(5) Å; $\text{Na}-\text{N5}$: 2.430(5) Å) and such a bonding generates a chain running in a -direction. Such chains are further connected to each other via H-bonds involving O_{amide} and pyridyl-H atoms resulting into a 2D network. The involvement of appended thiazoline rings in coordination to Na^+ ions immediately suggest the potential of **1** as a metalloligand for the synthesis of extended architectures.



Scheme 1. Synthetic route for metalloligand **1**. Conditions: (i) 2 equiv. NaH , DMF, N_2 ; (ii) 0.5 equiv. $[\text{Co}(\text{H}_2\text{O})_6](\text{ClO}_4)_2$; (iii) excess O_2 .

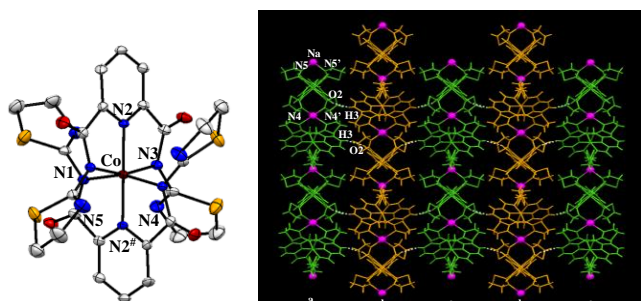
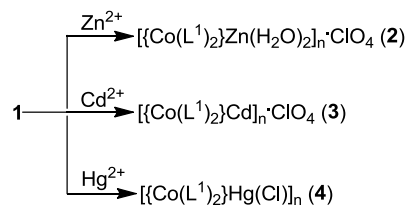


Figure 1. Thermal ellipsoidal representation of metalloligand **1** (left panel); thermal ellipsoids are drawn at 30% probability level whereas Na^+ ion and hydrogen atoms have been omitted for clarity. A packing view along the b axis (right panel); complex anions are shown in green and orange whereas the Na^+ ions are shown as magenta spheres. See text for details.

Synthesis and characterization of HCPs 2 – 4

The reaction of metalloligand **1** with $\text{Zn}(\text{II})$, $\text{Cd}(\text{II})$ and $\text{Hg}(\text{II})$ salts resulted in the isolation of heterometallic coordination polymers (HCPs) **2**, **3** and **4**, respectively (Scheme 2). The FTIR spectra of HCPs **2** – **4** exhibit ν_{amide} stretches between 1622-1630 cm^{-1} ; which are red-shifted (5–15 cm^{-1}) when compared to metalloligand **1**.^{18,21,25a} The diffuse-reflectance absorption spectra show λ_{max} at ca. 670 nm for all three HCPs (Fig. S4, ESI). The X-ray powder diffraction (XRPD) patterns of the three HCPs are in close match to those simulated from the single-crystal structures (Fig. S5 – S7, ESI). This fact asserts phase purity of bulk samples; although minor differences observed in diffraction line intensities can be attributed to the variation of the preferred orientation of crystallites in the powdered samples.^{20b,c} All three HCPs were investigated by the thermal gravimetric analysis (TGA) to shed light on the fate of coordinated and/or lattice solvent molecules and their thermal stability (Fig. S8, ESI). HCP **2** exhibits weight loss for two coordinated and two lattice water molecules (obs. 7.4%; calc. 7.5%) Similarly, HCPs **3** (obs. 5.8%; calc. 5.4 %) and **4** (obs. 4.0%; calc. 3.6%) display weight losses for three and two lattice water molecules, respectively. In all three cases, presence of coordinated and/or lattice solvent molecules is well-supported by the microanalysis data.



Scheme 2. Synthetic routes showing the reaction of metalloligand **1** with Zn^{2+} , Cd^{2+} and Hg^{2+} salts that produce HCPs **2** – **4**.

Crystal structures of HCPs 2 – 4

All three HCPs were crystallographically characterized to understand the coordination ability of metalloligand **1** towards the secondary metal ions. Metalloligand **1** offers four appended thiazoline rings available to further coordinate the secondary metal ions and the crystal structures of all three HCPs display their involvement in bonding. The central Co^{3+} ion displays an octahedral geometry within a N_6 coordination environment in all HCPs, as also noted in the crystal structure of metalloligand **1** (Table S1-S3). In a HCP, Co^{3+} core remains largely geometrically unaffected as observed for our pyridine and thiazole appended metalloligands.^{18,21-22} Such a fact suggests modular nature of the appended thiazoline rings in **1** that adjust to the steric and electronic requirements of the assorted secondary metal.

Crystal structure of HCP **2** exhibits the generation of a one-dimensional (1D) chain wherein metalloligands coordinate to the Zn^{2+} ions via $N_{\text{thiazoline}}$ and O_{amide} atoms (Fig. 2). The $\text{Zn}(\text{II})$ ion exhibits octahedral geometry in which two $N_{\text{thiazoline}}$ (N9 and $\text{N9}^{\#}$) and two O_{amide} (O3 and $\text{O3}^{\#}$) atoms constitute the N_2O_2 basal plane

whereas axial coordination sites are occupied by the water molecules (O8 and O8[#]). Importantly, both uncoordinated thiazoline rings are nicely arranged to make *intramolecular* H-bonds with the coordinated water molecules with O...N separations close to ca. 2.80 Å. The solid-state packing displays that the individual 1D chains are connected to each other via H-bonds between O_{amide} (O4) of one chain to that of thiazoline-H atom (H9a) of the second chain. Such packing is further strengthened due to H-bonding involving ClO₄⁻ ion (Fig. S9, ESI).

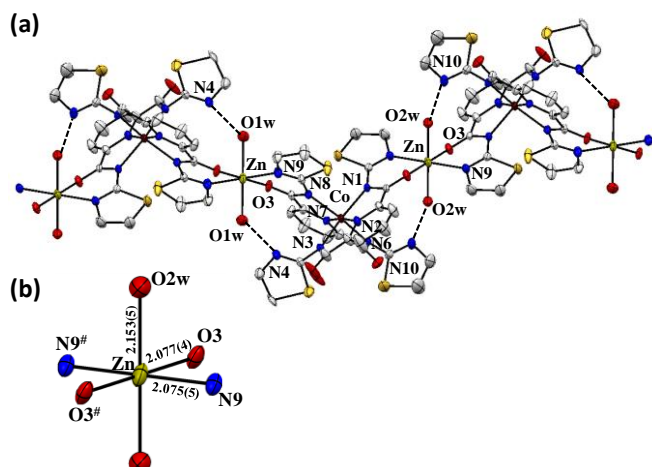


Figure 2. (a) Thermal ellipsoidal representation of HCP 2; thermal ellipsoids are drawn at 30% level whereas hydrogen atoms involved in hydrogen bonding are only shown for clarity. (b) Coordination sphere of Zn(II) ion with bond distances.

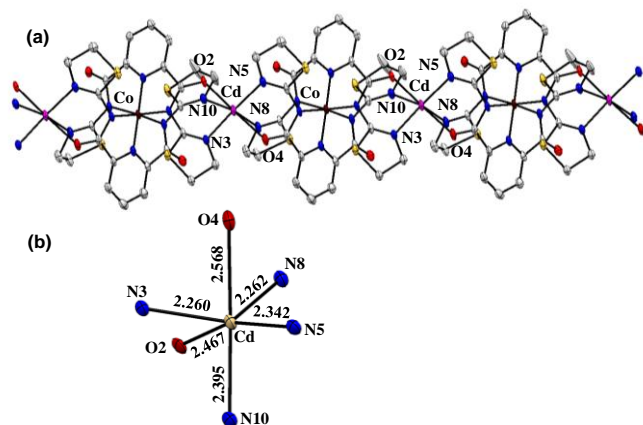


Figure 3. (a) Thermal ellipsoidal representation of HCP 3; thermal ellipsoids are drawn at 30% probability level whereas anion, solvent molecule and hydrogen atoms have been omitted for clarity. (b) Coordination sphere of Cd(II) ion with bond distances.

HCP 3 crystallizes in triclinic cell with *P*-1 space group. The crystal structure, similar to 2, shows the generation of a 1D chain where metalloligands are connected through Cd(II) ions (Fig. 3). Every Cd(II) ion displays a distorted octahedral geometry coordinated by four N_{thiazoline} atoms (2.260–2.395 Å) and two O_{amide} atoms (2.467 and 2.568 Å). The tentative basal plane around the Cd ion is constituted of N₃O atoms with axial sites occupied by N_{thiazoline} and O_{amide} atoms. In an individual

1D chain, O_{amide} atoms (O1 and O3) and thiazoline-H atoms from two metalloligands (H8a and H25b) show intra-chain H-bonding interactions. Such individual chains are further connected via inter-chain H-bonding involving O2_{amide} of one chain to that of thiazoline-H atoms (H12a and H22a) from the second chain thus generating 2D sheets of parallel running chains. A further inspection displays that such 2D sheets are interconnected to each other via ClO₄⁻ ions and lattice methanol molecules producing a 3D architecture (Fig. S10–S11, ESI).

HCP 4 crystallizes in trigonal cell with *R*-3 space group. The crystal structure, similar to 2 and 3, exhibits the generation of a 1D chain in which metalloligands are connected through the Hg(II) ions (Fig. 4a). In HCP 4, Hg(II) ion exhibits a severely distorted five-coordinate geometry (Fig. 4b) where four coordination sites are occupied by the thiazoline groups while the fifth one comes from a Cl⁻ ion (2.345 Å). Importantly, crystal structure displays uniqueness of the thiazoline rings. It was noted that the Hg(II) ion displays two short (avg. 2.278 Å) and two very long (avg. 2.691 Å) bonds from the thiazoline rings. A closer look establishes that two out of the four appended thiazoline rings per metalloligand were actually flipped to coordinate the Hg²⁺ ion through thiazoline-S atoms. Thus, effectively, every Hg(II) ion receives two shorter coordinations from the thiazoline-N donors (avg. 2.278 Å) and two longer ones from thiazoline-S atoms (avg. 2.691 Å). Such a bonding behavior adequately illustrates the tendency of a soft metal ion, Hg(II), to make a bond with a soft S donor.

HCP 4 displays an interesting solid-state packing in the form of hexagonal honeycomb architecture (Fig. 4c and S12, ESI). When viewed from the top, six 1D {Co³⁺-Hg²⁺} chains (shown in different colours in Fig. 4c) arrange to constitute a hexagonal ring. In a hexagonal ring, such 1D chains interact with each other via intermolecular H-bonding involving O_{amide} atoms (O2 and O3) and hydrogen atoms of thiazoline (H12b) and pyridine (H16) rings. Hexagonal rings are further connected to each other through H-bonds involving O4_{amide} and pyridine-H3 synthons generating a honeycomb structure.

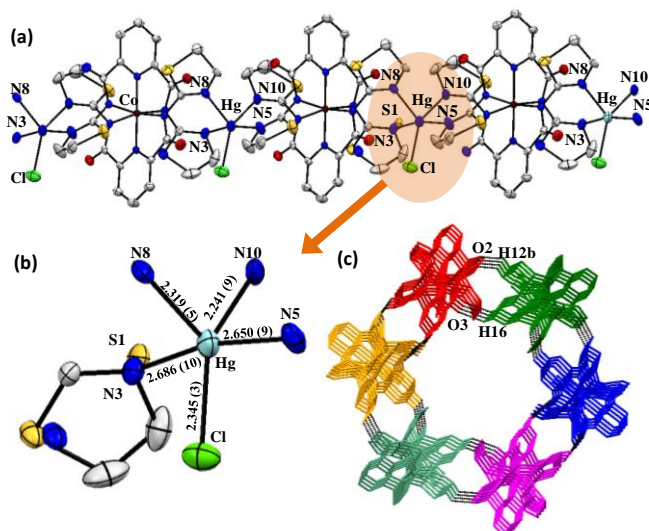


Figure 4. (a) Thermal ellipsoidal representation of HCP **4**; thermal ellipsoids are drawn at 30% probability level whereas hydrogen atoms have been omitted for clarity. (b) Coordination sphere of Hg(II) ion with bond distances including rotationally disordered thiazoline ring with both N and S atoms. (c) Honeycomb structure generated due to several weak interactions between 1D chains; see text for details.

Catalytic potentials of HCPs

Structural investigations of the three HCPs reveal the presence of Lewis acidic metal ion strongly coordinated by the thiazoline rings; however, weakly coordinated either by water molecule(s), O_{amide} atoms, or chloride ion. Such a bonding pattern suggests that the weakly coordinated atom/group could be easily replaced by a suitable substrate.^{19,22} This situation may therefore aid towards favourable interaction of substrate to the secondary metal and assist in its activation and thus catalysis.²² In addition, infinite dimension of HCPs results in their insolubility in common organic solvents, therefore, providing an option to carry out the catalytic reactions heterogeneously. Importantly, the present HCPs offer an excellent opportunity to carry out comparative catalytic reactions and evaluate the suitability of various secondary metal ions in such reactions. We anticipated that the relative size and Lewis acidity of a secondary metal ion may display preferential interaction towards substrates and such a difference may control the product outcome.^{18b,27} To illustrate such a feat; the focus of the catalysis is not towards high yield and/or high turnover number but to understand the reactivity difference between the three HCPs and more importantly, difference induced by the unique secondary metal ions on the catalysis.²⁷ Therefore, comparative catalysis experiments were carried out with the three HCPs. We selected ring-opening reactions (RORs), Knoevenagel condensation reactions (KCRs), and cyanation reactions (CRs) as these reactions are not only important for the production of fine chemicals but are known to be carried out effectively using a suitable Lewis acidic metal.^{18a,18b}

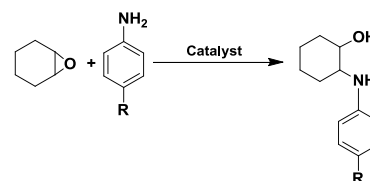
Ring-opening reactions. RORs of oxiranes and thiiranes with various nucleophiles are of immense interest due to the importance of such products in chemical and pharmaceutical research.²⁸ Activation of an oxirane/thiirane ring is a prerequisite condition for such a reaction and assorted reagents including Lewis acidic metal salts have been frequently used for such a purpose.^{18a,18b,29} Interestingly, compared to well-established RORs of oxiranes, similar reactions involving thiiranes as the substrates have been scarcely developed.^{18b,30} Such a stark difference is probably due to the tendency of thiiranes to undergo polymerization.^{30a} Hence, there is a requirement of a common catalyst that can effectively perform RORs of both oxiranes and thiiranes. In addition, performing such reactions heterogeneously remains a challenge despite practical significance.

All three HCPs were tested for the RORs of a few oxiranes and thiiranes using substituted anilines as the nucleophiles. To minimize competition from the solvent molecules and facile

isolation of products and separation of catalyst; solvent-free reaction conditions were employed. Under these reaction conditions, all three HCPs functioned as the heterogeneous catalysts. Thus, when cyclohexene oxide was treated with aniline in presence of only 2-mol % of any of the HCPs; a smooth reaction took place and the corresponding β -amino alcohol was obtained in good yield (Table 1). Reactions involving aniline as well as assorted *para*-substituted anilines containing both electron-donating and electron-withdrawing groups afforded the corresponding β -amino alcohols in good to high yield. Interestingly, HCP **3** was found to be the best catalyst whereas **4** was the least effective. We tentatively suggest that a subtle balance of ionic radius and Lewis acidity of Cd²⁺ ion, compared to Zn²⁺ (small size) and Hg²⁺ ion (lower Lewis acidity) allows cadmium metal to not only activate the epoxide ring but also orient the nucleophile before its attack, is the major reason for this difference.

To further analyse the catalytic abilities of three HCPs, RORs of cyclohexene sulfide was carried out using substituted anilines under the identical reaction conditions as mentioned for the cyclohexene oxide (Table 2). Satisfyingly, cyclohexene sulfide also reacted smoothly with aniline or substituted anilines producing the respective *trans*-2-phenylaminocyclohexanethiol. Interestingly, Hg-based HCP **4** was found to be the best catalyst out of three HCPs. We propose that the high affinity of Hg(II) ion to interact with the soft sulphur atom is the primary reason for the better performance of HCP **4**. Such an Hg²⁺...S interaction activates the thiirane ring effectively and enables the ROR in an efficient manner. The support for this hypothesis comes from the crystal structure of HCP **4** where Hg(II) ion displays coordination from S_{thiazole} in addition to N_{thiazole} groups. Such a fact adequately confirms the tendency of a soft metal ion, Hg(II), to interact with a soft S donor.

Table 1. Ring-opening reactions of cyclohexene oxide with aniline and *para*-substituted anilines using HCPs **2**, **3** and **4** as the catalysts.^[a]

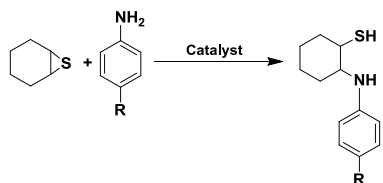


S. No.	R	Yield % ^[b]		
		2	3	4
1	-H	83, 82 ^[c] , 80 ^[d]	96, 93 ^[c] , 90 ^[d]	52
2	-C ₂ H ₅	88	97	72
3	-OCH ₃	85	92	65
4	-F	88	95	60
5	-Cl	82	94	62

[a] Reaction conditions: Catalyst – 2 mol%; Solvent-free reaction; 25 °C; 4

h stirring. [b] Yield was calculated from the GC. [c] Isolated yield for the third run with reused catalyst. [d] Isolated yield for the fourth run with reused catalyst.

Table 2. Ring-opening reactions of cyclohexene sulfide with aniline and *para*-substituted anilines using HCPs **2**, **3** and **4** as the catalysts.^[a]

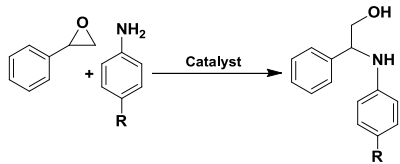


S. No.	R	Yield % ^[b]		
		2	3	4
1	-H	62, 60 ^[c] , 58 ^[d]	72, 70 ^[c] , 68 ^[d]	92, 90 ^[c] , 88 ^[d]
2	-C ₂ H ₅	71	70	94
3	-OCH ₃	75	72	90
4	-F	70	70	85
5	-Cl	78	75	90

[a] Reaction conditions: Catalyst – 2 mol%; Solvent-free reaction; 25 °C; 4 h stirring. [b] Yield was calculated from the GC. [c] Isolated yield for the third run with reused catalyst. [d] Isolated yield for the fourth run with reused catalyst.

To illustrate the effectiveness of the present HCPs to control the regioselectivity, styrene oxide was used as a representative unsymmetrical substrate (Table 3).^{18a,18b,19-20} Interestingly, a single product was obtained in all cases, therefore, suggesting a good control over the regioselectivity.³¹ Despite the fact that a nucleophile (*i.e.* aniline) could attack either at the benzylic carbon atom or at the less-hindered carbon atom of the substrate; in every case, nucleophile attack took place at the benzylic carbon atom affording a single product.³¹ A compelling proof came from the mass spectrum of the reaction which showed the characteristic molecular ion peak at m/z [M⁺-31] due to the loss of CH₂OH fragment.^{20,31a} This reaction indicates that the epoxide ring interacted with the catalytic secondary metal ion through the less-hindered side probably due to the steric reasons. The results exhibit the better catalytic performance of HCP **3** when compared to the other two HCPs as also noted in the ROR of cyclohexene oxide.

Table 3. Ring-opening reactions of styrene oxide with aniline and *para*-substituted anilines using HCPs **2**, **3** and **4** as the catalysts.^[a]



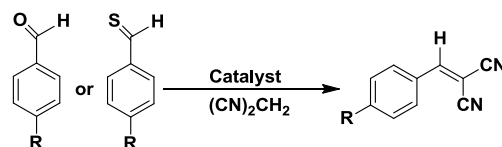
S. No.	R	Yield % ^[b]
--------	---	------------------------

		2	3	4
1	-H	75	90, 87 ^[c] , 86 ^[d]	65
2	-C ₂ H ₅	77	92	55
3	-OCH ₃	76	86	68
4	-F	81	91	52
5	-Cl	78	84	70

[a] Reaction conditions: Catalyst – 2 mol%; Solvent-free reaction; 25 °C; 4 h stirring. [b] Yield was calculated from the GC. [c] Isolated yield for the third run with reused catalyst. [d] Isolated yield for the fourth run with reused catalyst.

Knoevenagel condensation reactions. Reactions involving carbon-carbon bond formation are notable in the synthesis of fine chemicals. Knoevenagel condensation reaction (KCR) is one of such reactions which is known to produce several significant synthons and intermediates.³²⁻³⁴ We investigated the potential application of the three HCPs as the heterogeneous catalysts in the KCRs. In a typical reaction, benzaldehyde reacted cleanly with malononitrile in presence of only 2-mol% of HCPs (**2**, **3** and **4**) to produce 2-benzylidene-malononitrile as the only product. All three HCPs resulted in smooth reactions of several substituted benzaldehydes with malononitrile to afford the desired product in high yield (Table 4). The molecular size and/or the presence of electronic substituents does not seem to have considerable effect on the yield of the product.^{22,35} For example, sterically demanding 1- as well as 2-naphthaldehyde and 9-anthraldehyde produced the corresponding products in yield as good as noted for benzaldehyde suggesting the similar accessibility of substrate to the secondary metal ion.²² We then attempted similar reactions using substituted benzothialdehydes as the substrates to confirm if such substrates are activated better by any of the three HCPs.^{18b} Although the three HCPs produced the respective products in good yield; Hg-based HCP **4** was indeed more effective (compare entries 1, 3, and 6), therefore supporting our hypothesis.

Table 4. Knoevenagel condensation reactions of assorted aldehydes with (CN)₂CH₂ using HCPs **2**, **3** and **4** as the catalysts.^[a]



S. No.	R/Substrate	Yield %		
		2	3	4
1	-H	96(90) ^c	92(90) ^c	94(98) ^c
2	<i>m</i> -OCH ₃	94	93	85
3	<i>p</i> -OCH ₃	89(88) ^c	85(90) ^c	87(94) ^c
4	<i>m</i> -NO ₂	82	88	92

5	<i>p</i> -NO ₂	92	95	96
6	1-Naphthyl	88(85) ^c	85(88) ^c	89(92) ^c
7	2-Naphthyl	81	79	85
8	9-Anthryl	75	72	81

4	benzothialdehyde	75	84	90
5	4-methoxybenzothialdehyde	83	85	95
6	naphthalene-1-carbothialdehyde	62	75	85

[a] Reaction conditions: Catalyst–1 mol%; Solvent-free reaction; 25 °C; 4 h stirring. [b] Yield was calculated from the GC.

[a] Reaction conditions: Catalyst – 2 mol%; Solvent-free reaction; 25 °C; 4 h stirring. [b] Yield was calculated from the GC. [c] Numbers in parenthesis correspond to the respective sulphur analogue.

Cyanation reactions. With promising results for RORs and KCRs; HCPs **2** – **4** were further tested for CRs. CRs of carbonyl-based substrates provide a convenient route to cyanohydrins which are important intermediates for numerous chemicals.³⁵ Considerable efforts have been invested to design Lewis acid based catalysts, particularly heterogeneous catalysts incorporating Lewis acidic sites, for CRs.^{19-20,36} In this context, present HCPs appeared to be good candidates. As illustrated in Table 5, all three HCPs were able to catalyze CRs of assorted aldehydes using (CH₃)₃SiCN as the cyanide source. Benzaldehyde as well as assorted substituted analogues provided the corresponding cyanohydrins in good to excellent yield. Notably, even sterically demanding 1-naphthaldehyde was smoothly converted to its respective cyanohydrin which suggests that the size-selectivity is not a criterion.²² We tentatively suggest that the catalysis is occurring via activation of aldehyde before its reaction with cyanide. In order to prove such a postulation, HCP **2** was used as a representative example and impregnated with benzaldehyde and 1-naphthaldehyde by suspending crystals in a CH₂Cl₂ solution of such substrates. Such impregnated samples displayed considerable red-shift of C=O stretches for both aldehydes. For example, such stretches were shifted from 1705 to 1690 cm⁻¹ for benzaldehyde and from 1702 to 1690 cm⁻¹ for 1-naphthaldehyde (Fig. S13 and S14, ESI). Such an impregnation experiment adequately suggests activation of aldehydic substrate(s).^{20,22} While comparing the product yields for CRs, an important difference is quite evident; the yields are always on the higher side with Hg-based HCP whenever substrates are S-based. Such results, comparable to that of RORs of thiaranes, again strengthen our hypothesis that Hg-based HCP is better able to activates the S-based substrates.

Table 5. Cyanation reactions of assorted aldehydes (entry 1-3) and carbothioaldehyde (entry 4-6) with (CH₃)₃SiCN using HCPs **2**, **3** and **4** as the catalysts.^[a]

S. No.	R	Yield %		
		2	3	4
1	benzaldehyde	72	96	80
2	4-methoxybenzaldehyde	86	96	85
3	1-naphthaldehyde	84	92	80

Several groups have utilized assorted coordination polymers for various organic transformations, including ring-opening, cyanation and Knoevenagel condensation reactions.¹⁶ For example, Tanaka and co-workers³⁷ have used a Cu-based coordination polymer for the asymmetric RORs under the solvent-free conditions. In one such experiment, ROR of cyclohexene oxide with aniline showed 51% transformation with 51% enantiomeric excess. Garcia and coworker³⁸ have tested an iron-based coordination polymer for RORs of assorted epoxides with different nucleophiles (alcohols and amines). For example, styrene oxide on reaction with aniline at room temperature produces the corresponding ring-opened product in 52% yield. Bharadwaj and coworker³⁹ have used a Zn-based coordination polymer having Zn-bound labile water molecules for CRs and KCs. Using 5-mol% catalyst in CH₂Cl₂, 92% and 85% transformations were noted for CRs and KCs, respectively. These examples clearly suggest the superior nature of the present HCPs in the similar organic transformation reactions.

Recyclability and control experiments. KCRs were employed for recovering the HCPs and subsequently testing their stability and recyclability. All three HCPs could be easily recovered by simple filtration and were reused for carrying out KCRs of benzaldehyde with malononitrile for three consecutive catalytic cycles. It is important to mention that no purification or regeneration was used during the recyclability experiments. Gratifyingly, all three HCPs retained their catalytic efficiency throughout all such cycles. Such a fact is well-supported by the observation of superimposable FTIR spectra (Fig. S15 – S17; ESI) and powder XRD patterns (Fig. S18 – S20; ESI) of the recovered HCPs to that of as-synthesized samples. Both these studies assert that the crystallinity and structural integrity of the recovered material is preserved during the catalysis.

Control experiments further established that HCPs were essential for the catalysis as their removal during the reaction ceases the product formation. Figure S21 (ESI) illustrates such an experiment using HCP **2** where formation of 2-benzylidene-malononitrile was monitored using GC. As evident, there was no product formation after the removal of HCP **2**. However, re-adding **2** immediately causes the KCR to be resumed. This experiment therefore infers the *true* heterogeneous catalytic nature of HCP **2**. Finally, use of metalloligand **1** or a few M(II) salts as the catalysts (e.g., MCl₂ and M(OAc)₂) resulted in negligible product formation (< 5%) thus again justifying the catalytic impact of HCPs.

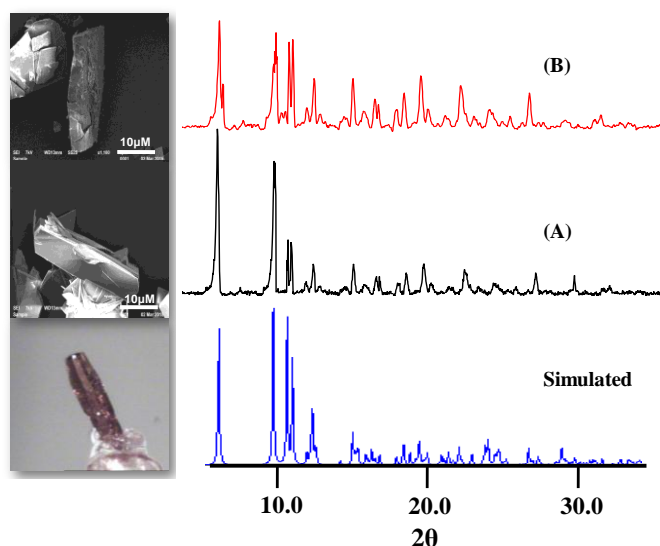


Figure 5. SEM micrographs (left panels) and XRPD patterns (right panels) of **2** (A) before and (B) after the KCRs. The bottom panel displays simulated XRPD pattern along with the optical photograph of the pristine sample.

We also attempted to understand the possible morphological changes to the crystalline HCPs during the course of catalysis. For such a study, HCP **2** was selected to carry out KCR of benzaldehyde with malononitrile. In a typical experiment, crystals of **2** were suspended in a mixture of benzaldehyde and malononitrile and were analysed by the powder XRD and scanning electron microscopic (SEM) images (Fig. 5). It is evident that the powder XRD patterns remain largely unchanged during the catalysis; however, SEM micrographs indicate minor changes which are noticeable from the cracks on the crystal surface. We therefore conclude that the present HCPs function as the efficient reusable heterogeneous catalysts for several Lewis acid assisted organic transformation reactions.

Conclusions

The present work has shown the synthesis of Zn^{2+} , Cd^{2+} and Hg^{2+} based heterometallic coordination polymers using metalloligand **1** offering appended thiazoline rings. The crystallographic studies substantiated the 1D infinite chain structures for all these coordination polymers. All three coordination polymers functioned as the heterogeneous and reusable catalysts for the ring-opening reactions of oxiranes and thiranes; Knoevenagel condensations of benzaldehydes and benzothialdehydes; and cyanation reactions of aldehydes and carbthialdehydes. The catalytic results illustrated that the structurally distinct secondary metal ions having different Lewis acidities potentially control the catalysis outcome via preferential interaction with the substrates.²⁷

Experimental

General

The reagents and chemicals were procured from the commercial sources and were used without further purification. The solvents were dried and/or purified using the standard literature methods.⁴⁰ The ligand H_2L^1 (N^2, N^6 -bis(4,5-dihydrothiazol-2-yl)pyridine-2,6-dicarboxamide) was synthesized as per our earlier report.^{22a}

Syntheses

Na[Co(L¹)₂] (1). Ligand H_2L^1 (0.50 g, 1.49 mmol) was dissolved in N_2 flushed DMF (10 mL) and treated with solid NaH (0.075 g, 3.129 mmol). The resulting solution was stirred for 30 min. at room temperature. Solid $[\text{Co}(\text{H}_2\text{O})_6](\text{ClO}_4)_2$ (0.272 g, 0.745 mmol) was added to the aforementioned solution followed by the bubbling of O_2 for 2 min. The solution was finally stirred for 1 h. The solution was filtered and the DMF was removed under the reduced pressure. The crude product was isolated after washing with diethyl ether. This product was re-dissolved in DMF and subjected to the vapor diffusion of diethyl ether that produced brown crystalline product within two days. Yield 0.8 g (72%). Anal. Calc. for $\text{C}_{26}\text{H}_{22}\text{N}_{10}\text{O}_4\text{S}_4\text{NaCo}\cdot 2\text{H}_2\text{O}$: C, 39.79; H, 3.34; N, 17.85; S, 16.34. Found: C, 39.72; H, 3.71; N, 17.61; S, 16.32. FTIR spectrum (KBr, selected peaks): 1618 (C=O) and 1559 (C=N) cm^{-1} . Molar conductivity (DMF ~ 1mM solution 298 K): $\Lambda_M = 70 \Omega^{-1} \text{cm}^2 \text{mol}^{-1}$. Absorption spectrum (λ_{max} , nm, DMF (ϵ , $\text{M}^{-1} \text{cm}^{-1}$)): 670 (140), 470 (sh, 1210). ^1H NMR spectrum (400 MHz, DMSO-d_6): $\delta = 8.39$ (t, $J=8.1$ Hz, 2H), 7.97 (d, $J=8.0$ Hz, 4H), 3.01 (t, $J=8.1$ Hz, 8H), 2.67 (t, $J=8.1$ Hz, 8H). ^{13}C NMR spectrum (100 MHz, DMSO-d_6): $\delta = 169.33$ (C₄), 161.60 (C₅), 156.30 (C₃), 139.86 (C₁), 123.90 (C₂), 58.03 (C₇), 32.89 (C₆).

[[Co(L¹)₂]Zn(H₂O)₂]_n·ClO₄ (2). Complex **1** (0.05 g, 0.066 mmol) was dissolved in MeOH (10 mL) followed by the addition of solid $\text{Zn}(\text{NO}_3)_2 \cdot x\text{H}_2\text{O}$ (0.04 g, 0.133 mmol). This caused precipitation of a product which was dissolved by the addition of a saturated aqueous solution of NaClO_4 (2 mL). The resulting solution was finally stirred for 2 h and passed through a pad of celtite in a medium porosity frit. To the filtrate, vapors of diethyl ether were diffused that produced red crystalline product within 3-4 d. Yield: 0.045 g (74%). Anal. Calc. for $\text{C}_{26}\text{H}_{26}\text{ZnCoN}_{10}\text{O}_{10}\text{S}_4\text{Cl}\cdot 2\text{H}_2\text{O}$: C, 32.44; H, 3.14; S, 13.32; N, 14.55. Found: C, 32.70; H, 2.83; S, 13.84; N, 15.12. FTIR spectrum (Zn-Se ATR, selected peaks): 1611, 1595 (C=O) and 1549 (C=N) cm^{-1} . Diffuse Reflectance Absorption Spectrum (λ_{max} , nm): 670.

[[Co(L¹)₂]Cd]_n·ClO₄ (3). This compound was synthesized in a similar manner as that of HCP **2** with following reagents: complex **1** (0.05 g, 0.066 mmol), $\text{Cd}(\text{NO}_3)_2 \cdot x\text{H}_2\text{O}$ (0.041 g, 0.133 mmol), and a saturated aqueous solution of NaClO_4 . Diffusion of diethyl ether vapors to the filtrate produced orange crystalline blocks within a day. Anal. Calc. for $\text{C}_{26}\text{H}_{22}\text{CoN}_{10}\text{O}_8\text{S}_4\text{ClCd}\cdot 3\text{H}_2\text{O}$: C, 31.49; H, 2.89; N, 13.40; S, 12.27. Found: C, 30.91; H, 2.45; N, 13.70; S, 11.39. FTIR spectrum (KBr, selected peaks) 1622 and 1594 (C=O), 1549 (C=N) cm^{-1} . Diffuse Reflectance Absorption Spectrum (λ_{max} , nm): 670.

$[\{\text{Co}(\text{L}^1)_2\}\text{Hg}(\text{Cl})]_n$ (**4**). Complex **1** (0.05 g, 0.066 mmol) was dissolved in 5 mL DMF followed by the layering of a MeOH solution (3 mL) of HgCl_2 (0.036 g, 0.133 mmol). The yellow-orange crystals appeared at the interface within a day were separated and dried in vacuum. Anal. Calc. for $\text{C}_{26}\text{H}_{22}\text{CoHgN}_{10}\text{O}_4\text{S}_4\text{Cl}_2\text{H}_2\text{O}$: C, 31.30; H, 2.63; N, 14.04; S, 12.85. Found: C, 31.54; H, 2.74; N, 14.18; S, 12.42. FTIR spectrum (Zn-Se, selected peaks): 1630 (C=O) and 1544 (C=N) cm^{-1} . Diffuse Reflectance Absorption Spectrum (λ_{max} , nm): 670.

Synthesis of carbothialdehydes.⁴¹ The respective aldehyde (1.0 eq.) was treated with Lawesson's reagent (1.5 eq.) in toluene and refluxed at 70 °C six for 8 h. The resulting pink colored solution was filtered and the solvent was removed under the reduced pressure. Oily remains were dissolved in diethyl ether and washed with water several times. Diethyl ether was removed to afford semi-solid compound. The isolated compounds displayed identical spectral features as reported in literature.⁴¹

Benzothialdehyde. Yield: 98%. FTIR spectrum (Zn-Se ATR, cm^{-1}): 916 (-C=S). 4-methoxybenzothialdehyde. Yield: 96%. FTIR spectrum (Zn-Se ATR, cm^{-1}): 910 (-C=S). MS: (ESI⁺, MeOH, m/z): calc. 153.0374 for 4-methoxybenzothialdehyde; found 153.0372 for $\text{M}+\text{H}^+$. Naphthalene-1-carbothialdehyde. Yield: 95%. FTIR spectrum (Zn-Se ATR, cm^{-1}): 910 (-C=S).

Catalytic Reactions

Cyanation Reaction. In a typical cyanation reaction, 1 mol% catalyst (**2**, **3** or **4**) was added to a mixture of carbaldehyde or carbothialdehyde (1 equiv.) and trimethylsilylcyanide (3 equiv.) and the reaction mixture was stirred at room temperature for 4 h.

Knoevenagel Condensation Reaction. In this reaction, 1 mol% catalyst (**2**, **3** or **4**) was added to a mixture of carbaldehyde or carbothialdehyde (1 equiv.) and malonitrile (1.5 equiv.) and the reaction mixture was stirred at room temperature for 4 h.

Ring-opening Reaction. 2 mol% catalyst was added to a mixture of oxirane or thiirane (1.0 equiv.) and aromatic amines (1.0 equiv.) and the reaction mixture was stirred at room temperature for 4 h.

General Procedure for catalytic reaction. In all cases, reactions were monitored either by thin-layer chromatography (TLC) and/or gas chromatography (GC). After the mentioned time, catalyst was filtered off and the filtrate was concentrated under reduced pressure. The crude product thus obtained was purified by flash column chromatography on silica gel using hexanes-ethyl acetate mixture (5:1) as the eluent. The product(s) were separated, isolated and analysed by GC, GC-MS, and NMR techniques. The recovered catalysts were washed with diethyl ether, dried and reused without further purification.

Physical measurements

The FTIR spectra were recorded either with the Perkin–Elmer FTIR-2000 or Spectrum–Two spectrometer having Zn-Se ATR. The NMR spectra were measured with a Jeol 400 MHz spectrometer. The absorption spectra were recorded either with Perkin–Elmer Lambda–25 or Perkin–Elmer Lambda–35 spectrophotometers. The conductivity measurements were carried out with a digital conductivity bridge from the Popular Traders, India (model number: PT 825). The elemental analysis data were obtained with an Elementar Analysen Systeme GmbH Vario EL-III instrument. Thermal gravimetric analysis (TGA) was performed with DTG 60 Shimadzu at 5 °C min^{-1} heating rate under the nitrogen atmosphere.

X-ray crystallography

Single crystal diffraction data for complexes **1** and **2** were collected on an oxford XCalibur CCD⁴² whereas for **3** and **4** on Bruker Kappa Apex-CCD diffractometer,^{43,44} respectively; equipped with graphite monochromatic $\text{Mo-K}\alpha$ radiation ($\lambda = 0.71073 \text{ \AA}$). The frames were collected at room temperature for **1**, **2**, and **4** and 100 K for **3**. The structures were solved by the direct methods with SIR-92⁴⁵ or SHELXS-97⁴⁶ and refined by the full-matrix least-squares refinement techniques on F^2 using the program SHELXL-97⁴⁶ incorporated in WINGX 1.8.05 crystallographic collective package.⁴⁷ Hydrogen atoms were fixed at the calculated position with isotropic thermal parameters whereas all non-hydrogen atoms were refined anisotropically. For **1**, high Ueq was observed for atom C13 which was successfully resolved by splitting it using PART command due to which the checkcif shows an A-level alert.

For **2**, disorder in the perchlorate ion could not be resolved and the refinement is done with restraints over Cl–O distances. Some disorder in the complex molecule was also seen which could only be resolved for one amide oxygen atom O2 and C9 of one of the thiazoline ring. These two atoms and C26 have been refined with restraints on their bond distances. The difference Fourier at this stage showed lots of scattered and diffuse electron density peaks having heights ranging between 4.50–1.08 $\text{e}\text{\AA}^3$ with some of them lying at two fold axis of rotation. These could not be modeled accurately, even by considering them disordered water molecules. So these were removed by using the SQUEEZE routine of PLATON.⁴⁸ The resultant model refined well and also improved on its *R* index. The SQUEEZE results show recovery of electrons which match well with one water molecule and 1–1.5 molecules of highly disordered DMF which was used as the solvent during crystallization and/or synthesis. The final model does not show any significant residual electron density peak. The model contains SAV of volume 266 \AA^3 because of the removed electron density.

For HCP **3**, disorder in ClO_4^- ion and a thiazoline ring was observed. Atoms Cl, O1, O2, O3 and O4 of ClO_4^- ion and C25 and C26 of thiazoline ring were occupying two crystallographic independent positions which could be located from the additional residual electron density. These atoms were modeled by splitting them at two positions while also applying restrains. This resulted in improved data convergence and meaningful

bond distances. However, some disordered electron density could not be resolved and thus corrected by using the SQUEEZE command of PLATON.⁴⁸ The electrons recovered correspond to 1-1.5 disordered DMF molecules. The model contains SAV of volume 154 Å³ because of the removed electron density.

In case of HCP **4**, the refinement showed disorder in some atoms (C12, C13, C25, C26, C21, C22, S1, S4 and N3) of the thiazoline rings. The thiazoline ring containing atoms S1 and N3 showed rotational disorder with both atoms sharing their position. These atoms were observed to occupy two different positions which were identified from the Fourier map. The disordered atoms were successfully modelled by fixing distances between the atoms by applying restraints. Further, atoms C13, C25, C26, C21, C22, and S4 were refined isotropically. For these atoms, site occupancy factors (SOFs) were refined with the help of free variable Part instruction. Refinement of the SOFs for disordered atoms gave the value 0.68. The structure shows large SAVs as a consequence of the crystal packing in absence of any other significant electron density. The crystallographic data collection and structure refinement parameters are presented in Table S4. CCDC 894199, 1059686 – 1059688 contain the supplementary crystallographic data for this paper. These data can be obtained free of charge from The Cambridge Data Center via www.ccdc.cam.ac.uk/data_request/cif.

Acknowledgements

RG gratefully acknowledges the financial support from the Science and Engineering Research Board (SERB), Govt. of India, New Delhi and the University of Delhi. Crystallographic data and instrumental facilities were provided by the CIF-USIC of this university. DB and SP respectively thank UGC and CSIR for their fellowships. Authors sincerely thank an anonymous reviewer for helping with the crystallographic work.

Notes and references

^aDepartment of Chemistry, University of Delhi, Delhi, 110 007, India. E-mail: rgupta@chemistry.du.ac.in; Fax: +91-11-2766 6605; Tel: +91-11-2766 6646 Ext. 172.

^bDepartment of Chemistry, Guru Nanak Dev University, Amritsar –143 005, Punjab, India.

†Electronic Supplementary Information (ESI) available: [Figures for NMR and absorption spectra, TGA plots, powder XRD patterns, weak interactions, inclusion studies, hot-filtration test; and crystallographic details and tables for bonding details and data collection]. See DOI: 10.1039/b000000x/

- G. Kumar, R. Gupta, *Chem. Soc. Rev.* 2013, **42**, 9403.
- a) R. Sessoli, A. K. Powell, *Coord. Chem. Rev.* 2009, **253**, 2328; b) M. Kurmoo, *Chem. Soc. Rev.* 2009, **38**, 1353; c) R. J. Kuppler, D. J. Timmons, Q.-R. Fang, J.-R. Li, T. A. Makal, M. D. young, D. Yuan, D. Zhao, W. Zhuang, H.-C. Zhou, *Coord. Chem. Rev.* 2009, **253**, 3042.

- a) R. Rasappan, D. Lanventine, O. Reiser, *Coord. Chem. Rev.* 2008, **252**, 702; b) D. MasPOCH, D. Ruiz-Molina, J. Veciana, *Chem. Soc. Rev.* 2007, **36**, 770.
- a) M. Andruh, D. G. Branznea, R. Gheorghe, A. M. Madalan, *CrystEngComm.* 2009, **11**, 2571; b) A.-I. Kamiyama, T. Konno, *Dalton Trans.* 2011, **40**, 7249.
- a) Y.Q. Sun, J. Zhang, Y.M. Chen, G.Y. Yang, *Angew. Chem. Int. Ed.* 2005, **44**, 5814; b) D.C. Zhong, M. Meng, J. Zhu, G.Y. Yang, T.B. Lu, *Chem. Commun.* 2010, **46**, 4354.
- a) R. Chakrabarty, P. S. Mukherjee, P. J. Stang, *Chem. Rev.* 2011, **111**, 6810; b) T. R. Cook, P. J. Stang, *Chem. Rev.* 2015, 0000; DOI: 10.1021/cr5005666.
- O. K. Farha, J. T. Hupp, *Acc. Chem. Res.* 2010, **43**, 1166.
- B. Chen, S. Xiang, G. Qian, *Acc. Chem. Res.* 2010, **43**, 1115.
- a) L. Pan, D.H. Olson, L.R. Ciemnomolowski, R. Heddy, J. Li, *Angew. Chem. Int. Ed.* 2006, **45**, 616; b) J.R. Li, R.J. Kuppler, H.C. Zhou, *Chem. Soc. Rev.* 2009, **38**, 1477.
- a) M.O'Keeffe, O. M. Yaghi, *Chem. Rev.* 2012, **112**, 675; b) D.J. Tranchemontagne, J.L. Mendoza-Corte's, M. O'Keeffe, O.M. Yaghi, *Chem. Soc. Rev.* 2009, **38**, 1257.
- a) C. K. Brozek, M. Dinca, *Chem. Soc. Rev.* 2014, **43**, 5456; b) P. Ramaswamy, N. E. Wong, G. K. H. Shimizu, *Chem. Soc. Rev.* 2014, **43**, 5913.
- a) S. Sen, N. N. Nair, T. Yamada, H. Kitagawa, P. K. Bharadwaj, *J. Am. Chem. Soc.* 2012, **134**, 19432; b) M. Sadakiyo, T. Yamada, H. Kitagawa, *J. Am. Chem. Soc.* 2014, **136**, 13166; c) M. Sadakiyo, T. Yamada, H. Kitagawa, *J. Am. Chem. Soc.* 2009, **131**, 9906.
- a) Z. Hu, B. J. Deibert, J. Li, *Chem. Soc. Rev.* 2014, **43**, 5815; b) V. Stavila, A. A. Talin, M. D. Allendorf, *Chem. Soc. Rev.* 2014, **43**, 5994; c) C. Wang, T. Zhang, W. Lin, *Chem. Rev.* 2012, **112**, 1084; d) M. D. Allendorf, C. A. Bauer, R. K. Bhakta, R. J. T. Houka, *Chem. Soc. Rev.* 2009, **38**, 1330; e) J. C. G. Bunzli, C. Piguet, *Chem. Rev.* 2002, **102**, 1897.
- a) X.N. Cheng, W.X. Zhang, Y.Y. Lin, Y.Z. Zheng, X.M. Chen, *Adv. Mater.* 2007, **19**, 1494; b) X.Y. Wang, Z.M. Wang, S. Gao, *Chem. Commun.* 2008, 281.
- a) J.H. Deng, X.L. Yuan, G.Q. Mei, *Inorg. Chem. Commun.* 2010, **13**, 1585; b) Q.Y. Yang, K. Li, J. Luo, M. Pan, C.Y. Su, *Chem. Commun.* 2011, **47**, 4234.
- a) L.Q. Ma, C. Abney, W.B. Lin, *Chem. Soc. Rev.* 2009, **38**, 1248; b) Liu, J.; Chen, L.; Cui, H.; Zhang, J.; Zhang, L.; Su, C.-Y. *Chem. Soc. Rev.* 2014, **43**, 6011; c) Dhakshinamoorthy, A.; Garcia, H. *Chem. Soc. Rev.* 2014, **43**, 5750; d) Corma, A.; Garcia, H.; Xamena, F. X. L. I. *Chem. Rev.* 2010, **110**, 4606; e) Lee, J. Y.; Farha, O. K.; Roberts, J.; Scheidt, K. A.; Nguyen, S. B. T.; Hupp, J. T. *Chem. Soc. Rev.* 2009, **38**, 1450.
- a) A. Ali, G. Hundal, R. Gupta, *Cryst. Growth. Des.* 2012, **12**, 1308; b) G. Kumar, H. Aggarwal, R. Gupta, *Cryst. Growth. Des.* 2013, **13**, 74; c) S. Srivastava, H. Aggarwal, R. Gupta, *Cryst. Growth. Des.* 2015, **15**, 4110; d) A. Ali, D. Bansal, R. Gupta, *J. Chem. Sci.* 2014, **126**, 1535.
- a) A. Mishra, A. Ali, S. Upreti, R. Gupta, *Inorg. Chem.* 2008, **47**, 154; b) A. Mishra, A. Ali, S. Upreti, M. S. Whittingham, R. Gupta, *Inorg. Chem.* 2009, **48**, 5234; c) A. P. Singh, R. Gupta,

- Eur. J. Inorg. Chem.* 2010, 4546; d) S. Srivastava, A. Ali, A. Tyagi, R. Gupta, *Eur. J. Inorg. Chem.* 2014, 2113.
- 19 a) G. Kumar, A. P. Singh, R. Gupta, *Eur. J. Inorg. Chem.* 2010, 5103; b) A. P. Singh, A. Ali, R. Gupta, *Dalton Trans.* 2010, 8135; c) A. P. Singh, G. Kumar, R. Gupta, *Dalton Trans.* 2011, 40, 12454; d) S. Srivastava, M. S. Dagur, R. Gupta, *Eur. J. Inorg. Chem.* 2014, 4966.
- 20 a) G. Kumar, R. Gupta, *Inorg. Chem.* 2012, 51, 5497; b) G. Kumar, R. Gupta, *Inorg. Chem.* 2013, 52, 10773; c) G. Kumar, G. Kumar, R. Gupta, *Inorg. Chem.* 2015, 54, 2603.
- 21 a) G. Kumar, R. Gupta, *Inorg. Chem. Commun.* 2012, 23, 103; b) G. Kumar, G. Kumar, R. Gupta, *Inorg. Chim. Acta* 2015, 425, 260.
- 22 a) D. Bansal, G. Kumar, G. Hundal, R. Gupta, *Dalton Trans.* 2014, 43, 14865; b) D. Bansal, G. Hundal, R. Gupta, *Eur. J. Inorg. Chem.* 2015, 1022.
- 23 a) R. A. Sheldon, J. K. Kochi, *Metal Catalyzed Oxidation of Organic Compounds*, Academic Press, New York, 1981; b) B. Meunier, *Biomimetic Oxidations Catalyzed by Transition Metal Complexes*, Imperial College Press, London, 2000; c) T. Zhang, M. Ozbil, A. Barman, T. J. Paul, R. P. Bora, R. Prabhakar, *Acc. Chem. Res.* 2015, 48, 192–200; d) T. B. Rauchfuss, *Acc. Chem. Res.* 2015, 48, 2107; e) L. P. Wolters, F. M. Bickelhaupt, *Chem. Asian J.* 2015, DOI: 10.1002/asia.201500368; f) B. Balakrishna, J. L. N. -Rico, A. V. Ferran, *Eur. J. Org. Chem.* 2015, 5293.
- 24 a) R. G. Pearson, *J. Am. Chem. Soc.* 1963, 85, 3533; b) D. P. N. Satchell, R. S. Satchell, *Chem. Rev.* 1969, 69, 251.
- 25 a) K. Nakamoto, *Infrared and Raman Spectra of Inorganic and Coordination Compounds*. Publishers, John Wiley & Sons, 1986; b) W. J. Geary, *Coord. Chem. Rev.* 1971, 7, 81.
- 26 J. L. Bricks, G. Reck, K. Rurack, B. Schlz, M. Spieless, *Supramol. Chem.* 2003, 15, 189.
- 27 It may be noted that the three HCPs offer unique coordination geometries of the secondary metal ions and such a factor may also contribute towards the catalytic difference.
- 28 a) W. Holderich, U. Barsnick, *Fine Chemicals Through Heterogeneous Catalysis*, Ed. R. A. Sheldon, H. van Bekkum, 2001, Wiley-VCH, Weinheim; b) C. J. Morten, A. J. Byers, A. R. Van Dyke, I. Vilotijevic, and T. F. Jamison, *Chem. Soc. Rev.* 2009, 38, 3175; c) K. B. Sharpless and T. R. Verhoeven, *Aldrichim. Acta* 1979, 12, 63.
- 29 a) J. Yamada, M. Yumoto, Y. Yamamoto, *Tetrahedron Lett.* 1989, 30, 4255; b) S. Sagawa, H. Abe, Y. Hase, T. Inaba, *J. Org. Chem.* 1999, 64, 4962; c) J. Auge, F. Leroy, *Tetrahedron Lett.* 1996, 37, 7715; d) M. Chini, P. Croti, L. Favero, M. Macchia, M. Pineschi, *Tetrahedron Lett.* 1994, 35, 433; e) T. Ollevier, G. Lavie-Compin, *Tetrahedron Lett.* 2004, 45, 49; f) L. R. Reddy, M. A. Reddy, N. Bhanumati, K. R. Rao, *Synthesis* 2001, 831; g) A. K. Chakraborti, A. Kondaskar, *Tetrahedron Lett.* 2003, 44, 8315; h) P. Q. Zhao, L. W. Xu, C. G. Xia, *Synlett.* 2004, 846; i) A. Kamal, R. Ramu, M. A. Azhar, G. B. R. Khanna, *Tetrahedron Lett.* 2005, 46, 2675.
- 30 a) M. Sander, *Chem. Rev.* 1966, 66, 297. (b) Q. Dong, X. Fang, J. D. Schroeder, D. S. Garvey, *Synthesis* 1999, 1106. (c) M. S. Reddy, K. Surendra, S. Krishnaveni, M. Narender, K. Rama Rao, K. *Helv. Chim. Acta* 2007, 90, 337. (d) H. Takeuchi, Y. Nakajima, *J. Chem. Soc. Perkin Trans. 2*, 1998, 2441.
- 31 a) Shivani, B. Pujala, A. K. Chakraborti, *J. Org. Chem.* 2007, 72, 3713; b) G. Mancilla, M. Femenia-Rios, J. Macias-Sanchez, I. G. Collado, *Tetrahedron*, 2008, 64, 11732.
- 32 a) F. Freeman, *Chem. Rev.* 1980, 80, 329; b) L. F. Tietze, *Chem. Rev.* 1996, 96, 115.
- 33 a) A. Lee, A. Michrowska, S. Sulzer-Mosse, B. T. List, *Angew. Chem. Int. Ed.* 2011, 50, 1707; b) Y. D. Wei, S. G. Zhang, S. F. Yin, C. Zhao, S. L. Luo, C. T. Au, *Catal. Commun.* 2011, 12, 1333; c) K. Ikeue, N. Miyoshi, T. Tanaka, M. Machida, *Catal. Lett.* 2011, 141, 877; d) A. C. Brooks, L. France, C. Gayot, J. Li, H. Pui, R. Sault, A. Stafford, J. D. Wallis, M. Stockenhuber, *J. Catal.* 2012, 285, 10; e) Y. Peng, J. Y. Wang, J. Long, G. H. Liu, *Catal. Commun.* 2011, 15, 10; f) G. Postole, B. Chowdhury, B. Karmakar, K. Pinki, J. Banerji, A. Auroux, *J. Catal.* 2010, 269, 110; g) D. Z. Xu, S. Shi, Yongmei Wang, *RSC Adv.* 2013, 3, 23075; h) R. J. Kalbasi, N. Mosaddegh, *Catal. Commun.* 2011, 12, 1231.
- 34 a) E. Merino, E. V. Sesto, E. M. Maya, M. Iglesias, F. Sánchez, A. Corma, *Chem. Mater.* 2013, 25, 981; b) D. Z. Xu, Y. J. Liu, S. Shi, Y. M. Wang, *Green Chem.* 2010, 12, 514; c) G. W. Li, J. Xiao, W. Q. Zhang, *Green Chem.* 2012, 14, 2234; d) Y. Tan, Z. Y. Fu, J. Zhang, *Inorg. Chem. Commun.* 2011, 14, 1966.
- 35 a) R. J. H. Gregory, *Chem. Rev.* 1999, 99, 3649; b) U. Muller, M. M. Schubert, O. M. Yaghi, *Handbook of Heterogeneous Catalysis*; Ed. G. Ertl, H. Knozinger, F. Schuth, J. Weitkamp, Wiley-VCH: Weinheim, Germany, 2008; c) M. North, *Tetrahedron: Asymmetry* 2003, 14, 147; d) J. M. Brunel and I. P. Holmes, *Angew. Chem. Int. Ed.* 2004, 43, 2752.
- 36 a) D. H. Ryu, E. J. Corey, *J. Am. Chem. Soc.* 2004, 126, 8106; b) J. M. Keith, E. N. Jacobsen, *Org. Lett.* 2004, 6, 153; c) Y. Hamashima, M. Kanai, M. Shibasaki, *J. Am. Chem. Soc.* 2000, 122, 7412; d) C. Baleizao, B. Gigante, H. Garcia, A. Corma, *Green Chem.* 2002, 4, 272.
- 37 K. Tanaka, S. Oda, M. Shiro, *Chem. Commun.* 2008, 820.
- 38 A. Dhakshinamoorthy, M. Alvaro, H. Garcia, *Chem. Eur. J.* 2010, 16, 8530.
- 39 S. Neogi, M. K. Sharma, P. K. Bharadwaj, *J. Mol. Catal. A-Chem.* 2009, 299, 1.
- 40 D. D. Perrin, W. L. F. Armarego, D. R. Perrin, *Purification of Laboratory Chemicals*, Pergamon Press, Oxford, 1980.
- 41 G. Minetto, L. F. Raveglia, A. Sega, M. Taddei, *Eur. J. Org. Chem.* 2005, 5277.
- 42 *CrysAlisPro*, ver. 1.171.33.49b (2009) Oxford Diffraction Ltd.
- 43 *SMART*: Bruker Molecular Analysis Research Tool, version 5.618, Bruker Analytical X-ray System, 2000.
- 44 *SAINT-NT*, Version 6.04, Bruker Analytical X-ray System, 2001.
- 45 A. Altomare, G. Cascarano, C. Giacovazzo, A. Guagliardi, *J. Appl. Crystallogr.* 1993, 26, 343.
- 46 G. M. Sheldrick, *Acta Cryst.* 2008, A64, 112.
- 47 L. J. Farrugia, WinGX version 1.64, An Integrated System of Windows Programs for the Solution, Refinement and Analysis of Single-Crystal X-ray Diffraction Data; Department of Chemistry, University of Glasgow, 2003.
- 48 A. L. Spek, PLATON, A Multipurpose Crystallographic Tool, Utrecht University, The Netherlands, 2002.

Graphical Abstract

Synopsis: Heterometallic coordination polymers function as the heterogeneous catalysts for various organic transformation reactions via preferential interaction with the substrates.

